Available online at www.sciencedirect.com
SCIENCE DIRECT®
Applied Surface Science xxx (2006) xxx–xxx
applied surface science
www.elsevier.com/locate/apsusc

Oleic acid coating on the monodisperse magnetite nanoparticles

Ling Zhang, Rong He, Hong-Chen Gu *

Institute for Micro and Nano Science and Technology, Shanghai Jiaotong University, 200030 Shanghai, China

Received 15 March 2005; received in revised form 27 December 2005; accepted 15 May 2006

Abstract

Monodisperse magnetite nanoparticles provide a more factual model to study the interface interactions between the surfactants and magnetic nanoparticles. Monodisperse magnetite nanoparticles of 7 and 19 nm coated with oleic acid (OA) were prepared by the seed-mediated high temperature thermal decomposition of iron(III) acetylacetonate ($Fe(acac)_3$) precursor method. Fourier transform infrared spectra (FTIR) and X-ray photoelectron spectroscopy (XPS) reveal that the OA molecules were adsorbed on the magnetic nanoparticles by chemisorption way. Analyses of transmission electron microscopy (TEM) shows the OA provided the particles with better isolation and dispersibility. Thermogravimetric analysis (TGA) measurement results suggest that there were two kinds of different binding energies between the OA molecules and the magnetic nanoparticles. The cover density of OA molecules on the particle surface was significantly various with the size of magnetite nanoparticles. Magnetic measurements of the magnetite nanoparticles show the surface coating reduced the interactions among the nanoparticles.

PACS: 73.20

Keywords: Monodisperse; Magnetite nanoparticles; Oleic acid; Chemisorption

1. Introduction

Magnetic nanoparticles have been of great interests because of their extensive applications in high-density data storage, biochemistry, hyperthermia, in vivo drug delivery, MR contrast reagent [1–7]. To apply magnetic nanoparticles in various potential fields, it is very important to control the size and shape, and to keep the thermal and chemical stability by surface modification [8]. This modification generally will play a key role on the properties and applications of the magnetic nanoparticles in bio-solutions or tissue environments [9]. The magnetic structure of the surface layer usually is greatly different from that in the body of nanoparticle, and the magnetic interactions in the surface layer could have a notable effect on the magnetic properties of nanoparticles [10,11]. Understanding the interaction between the surfactant and the nanoparticle is critical and essential to synthesis and application of nanoparticles.

Oleic acid (OA) is a commonly used surfactant to stabilize the magnetic nanoparticles synthesized by the traditional coprecipitation method, and some studies [12,13] have proved that the strong chemical bond formed between the carboxylic acid and the amorphous iron and amorphous iron oxide nanoparticles. However, it is hardly to know the interaction between the single nanoparticle and surfactant from the ''compositive'' results given by these kinds of size and shape widely dispersed nanoparticles systems. For the nanoparticles with different sizes, the surface effects are significantly various due to the difference of volume fraction of surface atoms within the whole particle. Excitingly, the chemical routes of synthesis monodisperse magnetic nanoparticles by thermal decomposition method have obtained outstanding results [14–17]. These monodisperse nanoparticles coated with OA may provide a factual system to get the exact information of the interaction and adsorption model at the interface. In the present work, monodisperse Fe_3O_4 nanoparticles with diameter of 7 and 19 nm were synthesized by the seed-mediated high temperature thermal decomposition of iron(III) acetylacetonate ($Fe(acac)_3$) precursor method. The chemical structure of the surfactant adsorbed on the magnetite nanoparticles has been identified, and the model of OA molecules adsorbed on the nanoparticles surface was discussed.

* Corresponding author. Tel.: +86 21 62933731; fax: +86 21 62804389.
E-mail addresses: zhangling_2003@sjtu.edu.cn (L. Zhang), hcgu@sjtu.edu.cn (H.-C. Gu).

0169-4332/$ – see front matter © 2006 Elsevier B.V. All rights reserved.
doi:10.1016/j.apsusc.2006.05.023

2. Experimental

Magnetite nanoparticles were prepared according to the Sun's method [16]. Such nanoparticles then serve as seeds to grow larger nanoparticles in the seed-mediated growth process. It is worth to note that the OA as the surfactant added in the reaction mixture before the Fe_3O_4 nuclei produced, but not as usual way that the surfactant was modified after the Fe_3O_4 synthesised [18–20].

In a typical synthesis, $Fe(acac)_3$ (2 mmol), 1,2-hexadecanediol (10 mmol), benzyl ether (20 ml), oleic acid (6 mmol), and oleylamine (6 mmol) were mixed and magnetically stirred under a flow of nitrogen. The mixture was heated to 200 °C for 30 min and then, under a blanket of nitrogen, heated to reflux (298 °C) for another 30 min. The black–brown mixture was cooled to room temperature by removing the heat source. After addition of ethanol and centrifuging, the monodisperse 7 nm Fe_3O_4 nanoparticles were obtained.

Such 7 nm Fe_3O_4 nanoparticles dispersed in hexane were used as seeds to grow larger Fe_3O_4 nanoparticles in the $Fe(acac)_3$ precursors solution. The mixture were first heated to 100 °C for 30 min to remove hexane, then to 200 °C for 1 h and keep at reflux (298 °C) for 1 h before being cooled down to room temperature. Following the workup procedures described in the synthesis of 7 nm Fe_3O_4 nanoparticles, the 19 nm Fe_3O_4 nanoparticles were obtained.

In order to perform the characterization of the sample, the as-synthesized magnetite nanoparticles were washed several times by ethanol to get rid of the ''free'' surfactant molecules and then were collected for drying to powder. To confirm the dryness of the samples, the samples were heated to 150 °C at a rate of 10 °C/min and maintained at that temperature for 2 h. If no mass loss (≤0.2%) was detected, we assumed that there was no remaining solvent in the sample.

2.1. Powder X-ray diffraction (XRD)

XRD were recorded on a Rigaku Dmax-r C X-ray diffractometer using Cu Kα ration (λ = 1.540 Å) operated at 40 KV and 100 mA.

2.2. Transmission electron microscopy (TEM)

The particle morphology, size and structure of the Fe_3O_4 were determined by Philips CM120 transmission electron microscopy operating at 80 kV. The two samples dispersed in the hexane were drop-cast onto the 300-mesh Formvar-covered copper grids separately.

2.3. High-performance particle sizer (HPPS)

Hydrodynamic diameter of magnetite nanoparticles were measured with a HPPS (Malvern Instrument, λ = 632.8 nm, T = 25 °C). The concentration of each sample was 3 mg Fe_3O_4/ml hexane.

2.4. Fourier transform infrared spectra (FTIR)

FTIR spectra of the nanoparticles were collected on a Bruker spectrometer. The sample powders were ground with KBr and compressed into a pellet whose spectra were record. A drop of neat OA was mixed with KBr and compressed into a pellet at 20000 psi, and the spectra were recorded as a reference.

2.5. X-ray photoelectron spectroscopy (XPS)

XPS analyses were performed with an ESCALAB-MK (VG Company). Photoemission was stimulated by a monochromated Al Kα radiation (1486.6 eV) with the operating at 12 kV and a 0.10 eV/step interval. Binding energies of spectra were referenced to the C 1s binding energy set at 284.6 eV. The samples powders were pressed to a pellet, and then the pellet was put into the entry-load chamber to pump for 4 h.

2.6. Thermogravimetric analysis (TGA)

Thermogravimetric analysis was carried out for powder samples (∼5 mg) with a heating rate of 10 °C/min using a Perkin-Elmer TGA 7 thermogravimetric analyzer in a synthetic N_2 atmosphere up to 800 °C.

2.7. Magnetic property measurement

The magnetic measurements were performed with a Quantum Design PPMS magnetometer and a vibrating sample magnetometer (VSM) (Lakeshore 7300) for the as-synthesis samples dispersed in octane and powders at room temperature, respectively.

3. Results and discussion

XRD patterns in Fig. 1 reveal the nanocrystal nature of the two samples. The position and relative intensity of all peaks

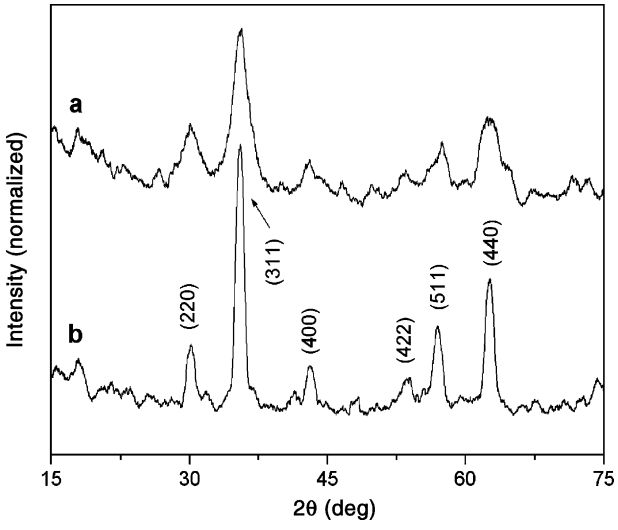

Fig. 1. The XRD diffraction pattern of (a) 7 nm seeds of as-synthesized Fe_3O_4 nanoparticles; (b) Fe_3O_4 nanoparticles with diameter of 19 nm.

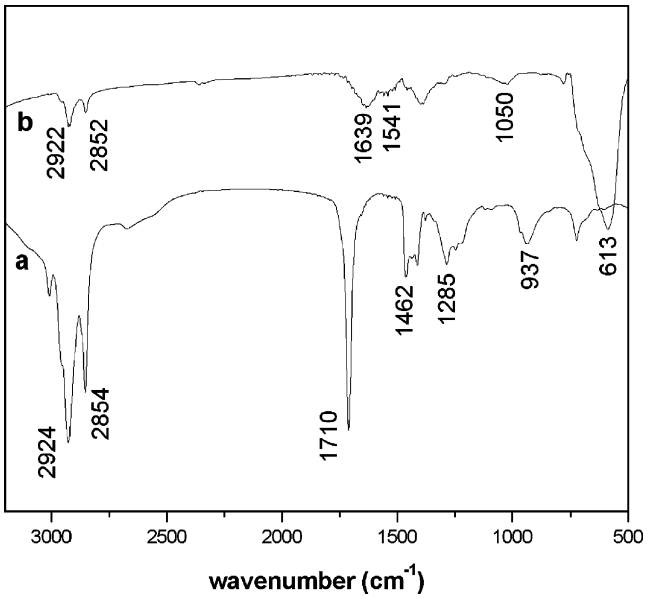

Fig. 2. FTIR spectra of (a) pure oleic acid; (b) Fe_3O_4 nanoparticles coated with oleic acid.

match well with standard Fe_3O_4 powder diffraction data, indicating that each sample is Fe_3O_4 crystal.

To understand the adsorption mechanism of the OA on the surface of Fe_3O_4 nanoparticles, Fourier transform infrared measurements were carried out on the pure oleic acid and the composite Fe_3O_4 nanoparticles coated with OA. Fig. 2 shows the typical FTIR spectrum of the pure oleic acid (a), and Fe_3O_4 nanoparticles coated with oleic acid (b). In curve (a), two sharp bands at 2924 and 2854 cm^{-1} were attributed to the asymmetric CH_2 stretch and the symmetric CH_2 stretch, respectively. The intense peak at 1710 cm^{-1} was derived from the existence of the C=O stretch, and the band at 1285 cm^{-1} exhibited the presence of the C–O stretch. The O–H in-plane and out-of-plane bands appeared at 1462 and 937 cm^{-1}, respectively. In the curve (b), the asymmetric CH_2 stretch and the symmetric CH_2 shifted to 2922 and 2852 cm^{-1}, respectively. The surfactant molecules in the adsorbed state were subjected to the field of the solid surface. As a result, the characteristic bands shifted to a lower frequency region which indicated that the hydrocarbon chains in the monolayer surrounding the nanoparticles were in a closed-packed, crystalline state [21]. It is worth to note that the C=O stretch band of the carboxyl group, which was present at 1710 cm^{-1} in the curve (a), spectrum of the pure liquid oleic acid, was absent in the curve (b), spectrum of the coated nanoparticles. And there appeared two new bands at 1541 and 1639 cm^{-1}, which were characteristic of the asymmetric ν_{as}(COO–) and the symmetric ν_s(COO–) stretch, instead. This result can be explained that the bonding pattern of the carboxylic acids on the surface of the nanoparticles was a combination of molecules bonded symmetrically and molecules bonded at an angle to the surface [22]. A strong adsorption at 1050 cm^{-1} arises from C–O single bond stretching. These results revealed that oleic acid were chemisorbed onto the Fe_3O_4 nanoparticles as a carboxylate.

Combined with previous studies of carboxylates, the interaction between the carboxylate head and the metal atom was categorized as four types: monodentate, bridging (bidentate), chelating (bidentate), and ionic interaction [21,23]. The wavenumber separation, Δ, between the ν_{as}(COO–) and ν_s(COO–) IR bands can be used to distinguish the type of the interaction between the carboxylate head and the metal atom. The largest Δ (200–320 cm^{-1}) was corresponding to the monodentate interaction and the smallest Δ (<110 cm^{-1}) was for the chelating bidentate. The medium range Δ (140–190 cm^{-1}) was for the bridging bidentate. In this work, the Δ (1639–1541 = 98 cm^{-1}) was ascribed to chelating bidentate, where the interaction between the COO– group and the Fe atom was covalent (as showed in Scheme 1).

The XPS spectra of C 1s, Fe 2p core level give a further proof for the chemical structure of the OA coated Fe_3O_4 nanoparticles in Fig. 3. Two C 1s peaks posited at 284.6 and 287.4 eV for 7 nm Fe_3O_4 nanoparticles, and 284.6 and 288.3 eV for 19 nm Fe_3O_4 nanoparticles. Peak at 284.6 eV was ascribed to the carbon atoms in the aliphatic chain (C–C), and peaks at 287.4 and 288.3 eV belonged to the carboxylate ($-COO^-$) moiety, which were consistent with the data obtained from carboxylateds in the previous literature [24]. C 1s peak corresponded to carboxylic carbon (–COOH), which posited at 290 eV, did not appear in the spectrum, indicating the absence of free acid on the coated Fe_3O_4 nanoparticles. The bonding energies at 710.8 eV were the characteristic peak from Fe $2P_{3/2}$ core level electrons. The Fe $2p_{1/2}$ peaks at 724.1 eV for 7 nm and 725.0 eV for 19 nm Fe_3O_4 nanoparticles were attributed to the carboxylate–Fe bond. The XPS results substantiate to the FTIR data, indicating the formation of chemical bonds between the iron oxide substrate and the oxygen atoms of the carboxylic acid.

Fig. 4 shows TEM images of magnetite nanoparticles coated with OA. The sizes of faceted particles were 7 nm for seeds, 19 nm for the nanoparticles synthesized by seed-mediated growth method. Each particle was separated from its neighbors by the organic ligands absorbed on the particles. It can be seen that the intervals of each neighboring Fe_3O_4 nanoparticles were uniform.

Dynamic laser scattering (DLS) had been performed as an additional method to determine the particle size and distribution. Fig. 5 gives the HPPS results of the as-synthesis samples. It is evident that this hydrodynamic diameter was larger than the size determined from TEM. The value of the hydrodynamic

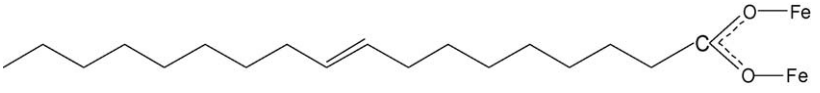

Scheme 1. Chelating bidentate interaction between the COO– group of oleic acid and the iron atom.

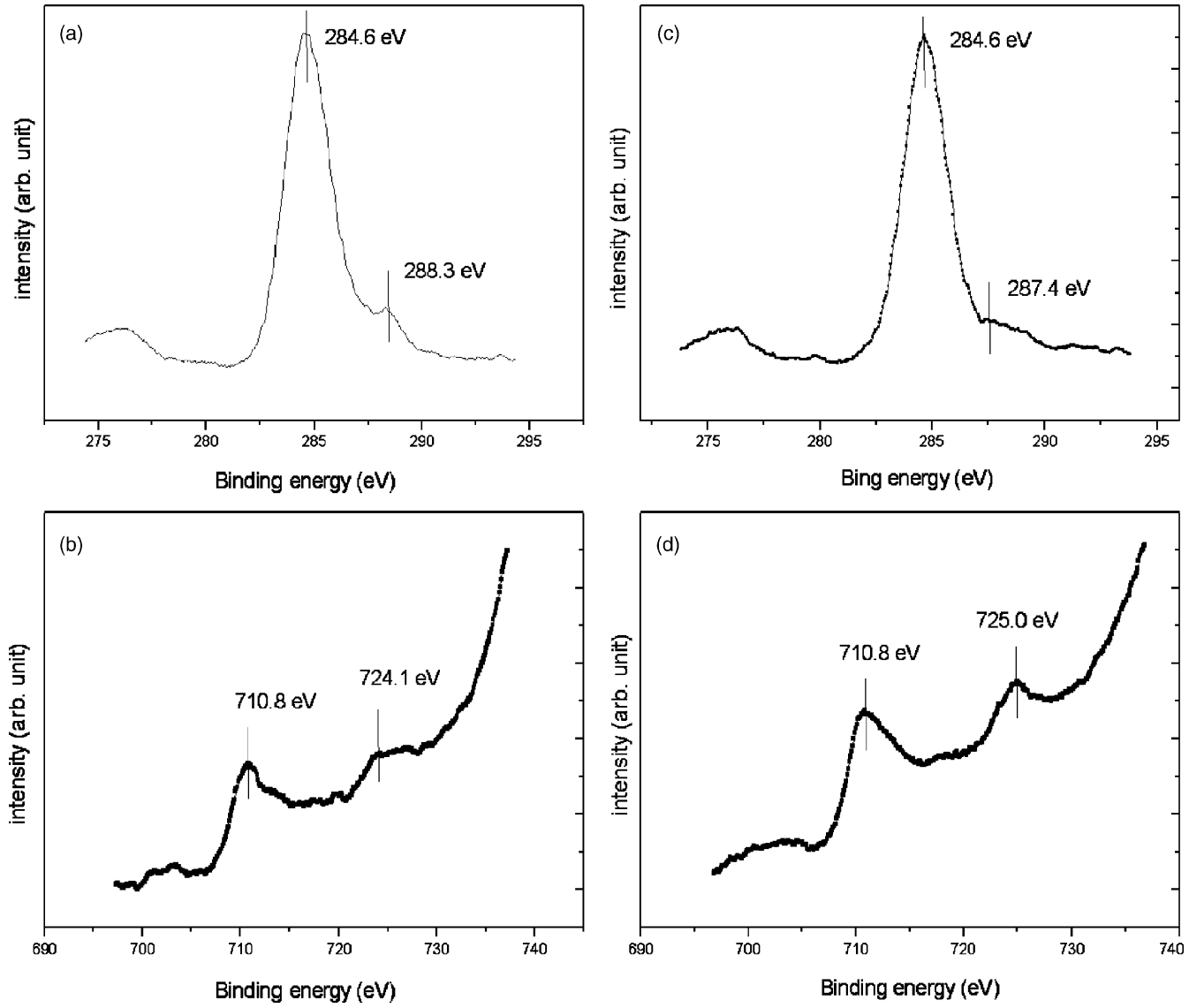

Fig. 3. XPS spectra obtained from the oleic acid coated Fe_3O_4 nanoparticles: (a) C 1s core level of 19 nm particles; (b) C 1s core level of 7 nm particles; (c) Fe 2p core level of 19 nm particles; (d) Fe 2p core level of 7 nm particles.

diameter was composed of size of the OA (2 nm) molecule and the magnetite nanoparticle ($D_{\text{hydrodynamic}} = D_{\text{TEM}} +$ 2 nm + 2 nm). The TEM and HPPS analysis showed the size and shape of as-synthesized Fe_3O_4 nanoparticles was homogenous. It indicated the marco-characterization may truly reflect the single nanoparticles information in this monodisperse system.

TGA derivative curves show two distinct transitions for both sizes samples between room temperature and 600 °C in Fig. 6. The transition temperatures and the corresponding percentage weight losses were summarized in Table 1. It is clear from the data that two desorption processes occured in the coated nanoparticles in the vicinity of 260 and 380 °C both in 7 and 19 nm nanoparticles. These different desorption processes were explained by the bilayer or quasi-two-layers adsorbed models on the particles surface previously [18,19]. But Gedanken and co-workers [25] found that the TGA of phosphate coated amorphous ferric oxide particles was double-stepped, and they attributed the results to two kinds of bonding of the phosphonate group on the Fe surface but rather a bilayer structure. Two types of bonding pattern on the surface was also suggested by Spencer and co-workers [26] for phosphate coated Ta_2O_5 and Hiroshi et al. [27] for $HCOOCH_3$ adsorbed on MgO surface. In this case, it is interesting to find that the ratio of the first weight loss to the second weigh loss was about 0.4:1 for both 7 and 19 nm Fe_3O_4 nanoparticles (Table 1). We think that there were two possible reasons to explain the constant ratio of two kinds of weight loss. First, in generally, the different surface shows different adsorption activity [28]. The as-synthesized Fe_3O_4 nanoparticle was terminated by (1 1 1) faces and (1 0 0) faces and the ratio of two faces may keep constant for both 7 and 19 nm Fe_3O_4 nanoparticles; second, the OA may be bonded with two states of iron ion. We plan to perform further study to confirm the detailed mechanism to explain the phenomenon. Consider the results from TGA HPPS, we confirm that there was a single oleic acid molecule layer

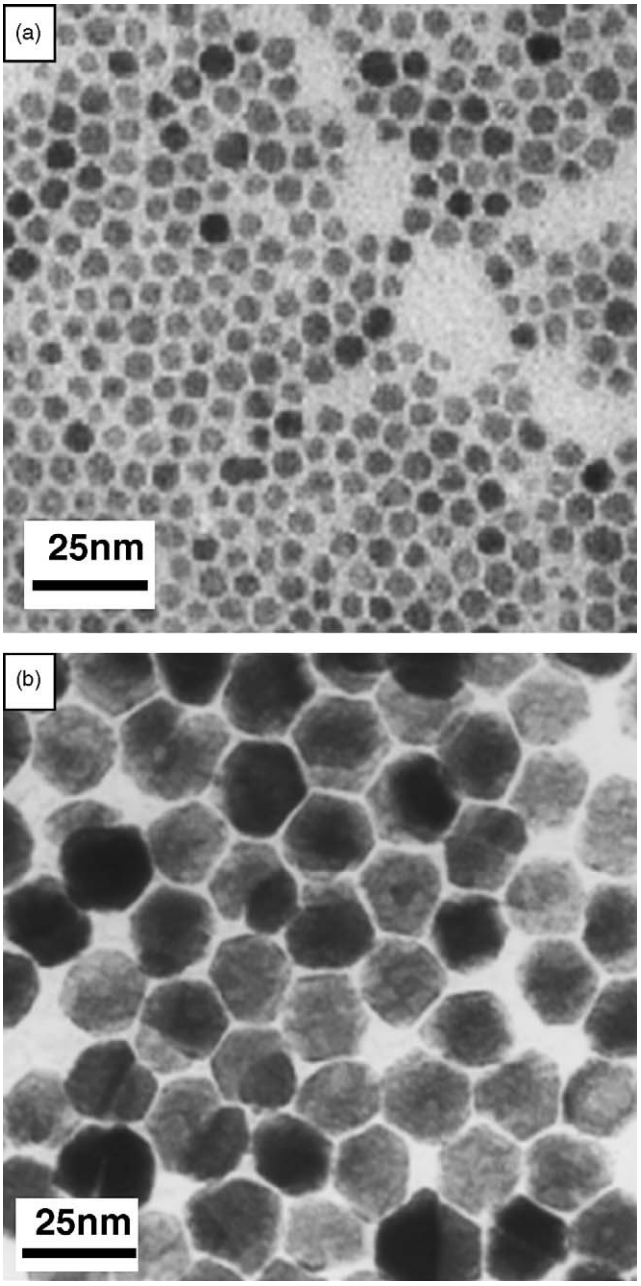

Fig. 4. TEM images of magnetite nanoparticles: (a) 7 nm seeds of as-synthesized Fe_3O_4 nanoparticles; (b) Fe_3O_4 nanoparticles with diameter of 19 nm.

adsorbed on the surface of the Fe_3O_4 nanoparticle, but the OA molecule adsorbed by two kinds of bonding energy.

Table 1 shows the surfactant adsorption amount decreased with the size of the Fe_3O_4 nanoparticles increasing. For 7 nm nanoparticles, the total amount was 25.1%, whereas as for 19 nm it was 6.5%. Based on the above single layer adsorption model, the cover density of OA molecular chemisorbed on the particle surface could be calculated from the TGA results. The cover density was 98% with the 7 nm nanoparticles, but dramatically decreased to 62% with diameter of 19 nm. The cover densities on the nanoparticle surfaces were decreased with the increasing of the nanoparticles sizes. This sharp difference between the two sizes of particles may result from

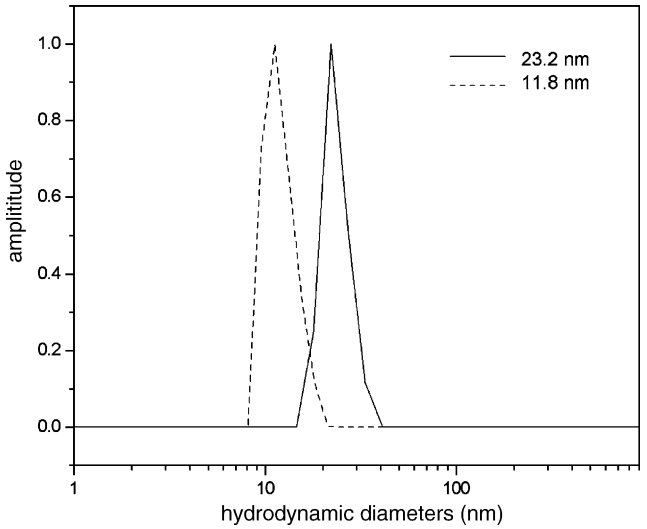

Fig. 5. HPPS results of 7 nm (- - -), 19 nm (—) Fe_3O_4 nanoparticles.

the balancing of Van der Waals energies and osmotic pressure. More surfactant molecules adsorbed on the smaller size particles increased the osmotic pressure (repulsion force) to balance the increasing Van der Waals energies (attraction) resulted from smaller size. The cover density comparison among various sizes of nanoparticles is meaningful for interpreting the solution of nanoparticles coated with surfactant. We find that the larger Fe_3O_4 nanoparticles were rather hard to re-disperse in the solvent after drying treatment but the smaller size of nanoparticles were well re-dispersed after the drying. Vastly differing coverage density would represent different surface environments and therefore will introduce uncertainty to the magnetic response of nanoparticles after the surface modification.

Fig. 7 displays the magnetization of coated Fe_3O_4 nanoparticles with different sizes which were dispersed in the solution or powder states at room temperature. In Fig. 7(b), the nature of the curves in both case show no coercivity,

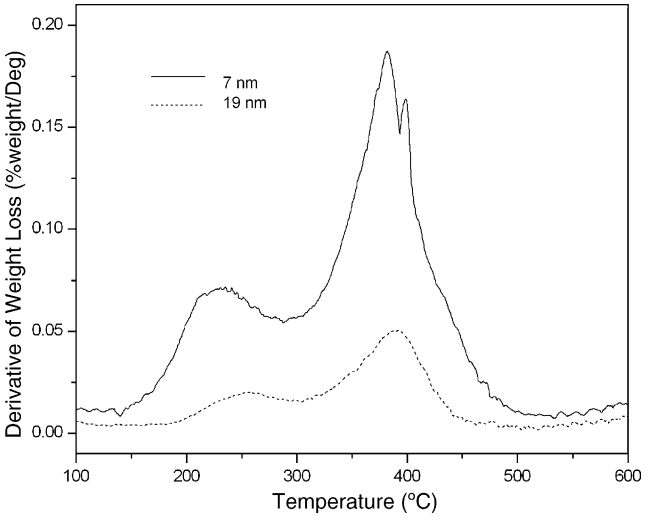

Fig. 6. TGA results: derivative of the weight loss as function of temperature for oleic acid coated Fe_3O_4 nanoparticles.

Table 1
Results and analysis based on TGA cures in Fig. 6

Sample size (nm)	TGA					
	First weight loss		Second weight loss			
	Derivative peak (°C)	Weight loss (%)	Derivative peak (°C)	Weight loss (%)	Total loss (%)	Packing density (%)*
7	261	7.5	382	17.6	25.1	98.0
19	256	1.9	391	4.6	6.5	62.0

* Packing density was calculated by total loss/coated surfactants × 100%, which it supposed that the area of the head of the oleic acid and oleic amine is 24 Å.

suggesting the superparamagnetic nature of the particles. However, the coercivity was appeared in the curve in Fig. 7(a). This phenomenon can explain that magnetic interactions between the particles should exist in these two samples since the particles have not been isolated in a matrix or fluid [29]. Consequently, the coated OA molecules on the particles surface can protect the Fe_3O_4 nanoparticles and reduce the interaction between the particles in the non-polar solution.

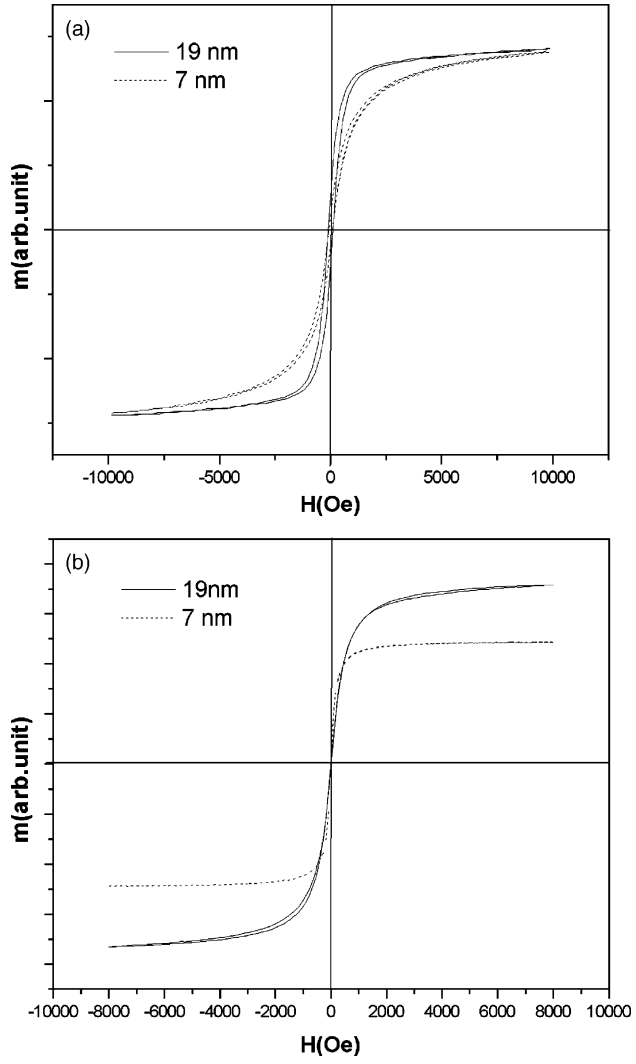

Fig. 7. (a) Hysteresis loop of the 7 and 19 nm Fe_3O_4 nanoparticles powders assembly measured at 300 K. (b) Hysteresis loop of the 7 and 19 nm Fe_3O_4 nanoparticles dispersed in hexane measured at 300 K.

4. Conclusions

Monodisperse magnetite nanoparticles coated with OA provided a factual system to get the exact information about the interaction and adsorption model at interface. Study shows the adsorption of OA molecules on the nanoparticles were by chemisorption in all cases, and the OA molecular coated on the particles surface with a single layer structure. Furthermore, the two distinct of surfactant desorbed on the particle surface implied that there were two kinds of different binding energies between the OA molecular and the particle surface. The total adsorption amount and cover density of OA molecular on the Fe_3O_4 nanoparticles surface decreased sharply with the increase of the sizes of the particles. Coated OA molecules can reduce the interactions between the Fe_3O_4 nanoparticles.

Acknowledgments

The authors are grateful to the 863 Hi-Tech Research and Development Program (2002AA302210) and Shanghai Nano Program (0249 nm071) for financial support.

References

[1] A.K. Gupta, A.S.G. Curtis, J. Mater. Sci.-Mater. Med. 15 (2004) 493.
[2] R. Hergt, R. Hiergeist, I. Hilger, W.A. Kaiser, Y. Lapatnikov, S. Margel, U. Richter, J. Magn. Magn. Mater. 270 (2004) 345.
[3] M. Johannsen, A. Jordan, R. Scholz, M. Koch, M. Lein, S. Deger, J. Roigas, K. Jung, S. Loening, J. Endourol. 18 (2004) 495–500.
[4] R.H. Kodama, J. Magn. Magn. Mater. 200 (1999) 359.
[5] G.X. Li, V. Joshi, R.L. White, S.X. Wang, J.T. Kemp, C. Webb, R.W. Davis, S.H. Sun, J. Appl. Phys. 93 (2003) 7557.
[6] H.B. Shen, Y.B. Wang, H.F. Yang, J.S. Jiang, Chin. Sci. Bull. 48 (2003) 2698.
[7] H. Zeng, J. Li, Z.L. Wang, J.P. Liu, S.H. Sun, Nano Lett. 4 (2004) 187.
[8] V.F. Puntes, K.M. Krishnan, A.P. Alivisatos, Science 291 (2001) 2115.
[9] D.K. Kim, M. Mikhaylova, Y. Zhang, M. Muhammed, Chem. Mater. 15 (2003) 1617.
[10] A.T. Ngo, P. Bonville, M.P. Pileni, Eur. Phys. J. B 9 (1999) 583.
[11] C.R. Vestal, Z.J. Zhang, J. Am. Chem. Soc. 125 (2003) 9828.
[12] N.Q. Wu, L. Fu, M. Su, M. Aslam, K.C. Wong, V.P. Dravid, Nano Lett. 4 (2004) 383.
[13] G. Kataby, M. Cojocaru, R. Prozorov, A. Gedanken, Langmuir 15 (1999) 1703.
[14] M. Chen, J.P. Liu, S.H. Sun, J. Am. Chem. Soc. 126 (2004) 8394.
[15] O. Song, Z.J. Zhang, J. Am. Chem. Soc. 126 (2004) 6164.
[16] S.H. Sun, H. Zeng, J. Am. Chem. Soc. 124 (2002) 8204.
[17] S.H. Sun, S. Anders, T. Thomson, J.E.E. Baglin, M.F. Toney, H.F. Hamann, C.B. Murray, B.D. Terris, J. Phys. Chem. B 107 (2003) 5419.

[18] Y. Sahoo, H. Pizem, T. Fried, D. Golodnitsky, L. Burstein, C.N. Sukenik, G. Markovich, Langmuir 17 (2001) 7907.
[19] L.F. Shen, P.E. Laibinis, T.A. Hatton, Langmuir 15 (1999) 447.
[20] L. Fu, V.P. Dravid, D.L. Johnson, Appl. Surf. Sci. 181 (2001) 173.
[21] K. Nakamoto, Infrared and Raman spectra of inorganic and coordination compounds, John Wiley & Son, New York, 1997.
[22] Y.T. Tao, J. Am. Chem. Soc. 115 (1993) 4350.
[23] Y. Ren, K. Iimura, T. Kato, Langmuir 17 (2001) 2688.
[24] E. Frydman, H. Cohen, R. Maoz, J. Sagiv, Langmuir 13 (1997) 5089.
[25] C. Yee, G. Kataby, A. Ulman, T. Prozorov, H. White, A. King, M. Rafailovich, J. Sokolov, A. Gedanken, Langmuir 15 (1999) 7111.
[26] M. Textor, L. Ruiz, R. Hofer, A. Rossi, K. Feldman, G. Hahner, N.D. Spencer, Langmuir 16 (2000) 3257.
[27] O. Hiroshi, E. Chikashi, A. Tetsuya, C. Yee, Surf. Sci. 191 (1987) 479.
[28] Z.L. Wang, Handbook of Nanophase and Nanostructured Materials-Characterization, Kluwer Academic Plenum Publishers, 2002.
[29] M.P. Morales, S. Veintemillas-Verdaguer, M.I. Montero, C.J. Serna, A. Roig, L. Casas, B. Martinez, F. Sandiumenge, Chem. Mater. 11 (1999) 3058.